Experimental method of detecting relic neutrino by atomic de-excitation

M. Yoshimura,[1,*] N. Sasao,[2,†] and M. Tanaka[3,‡]

[1]*Center of Quantum Universe, Faculty of Science, Okayama University, Tsushima-naka 3-1-1 Kita-ku Okayama 700-8530 Japan*

[2]*Research Core for Extreme Quantum World, Okayama University, Tsushima-naka 3-1-1 Kita-ku Okayama 700-8530 Japan*

[3]*Department of Physics, Graduate School of Science, Osaka University, Toyonaka, Osaka 560-0043, Japan*

(Received 14 September 2014; published 9 March 2015)

The cosmic background neutrino of temperature 1.9 K affects rates of radiative emission of neutrino pairs (RENP) from metastable excited atoms, since its presence blocks the pair emission by the Pauli exclusion principle. We quantitatively investigate how the Pauli blocking distorts the photon energy spectrum and calculate its sensitivity to cosmic parameters such as the neutrino temperature and its chemical potential. Important quantities for high sensitivities to these parameter measurements are found to be the level spacing of atomic deexcitation and the unknown mass value of the lightest neutrino, in particular, their relationship to one another.

DOI: 10.1103/PhysRevD.91.063516 PACS numbers: 98.80.Es, 13.15.+g, 14.60.Pq, 32.10.-f

The relic cosmic neutrino of temperature $(4/11)^{1/3}T_\gamma \sim 1.9$ K (with T_γ the cosmic microwave temperature) is undoubtedly one of the most important predictions of the big bang cosmology [1]. Detection of the relic neutrino would provide strong support for the nucleosynthesis theory that explains the origin of cosmic light elements such as ^{4}He. Various ideas of experimental methods of relic neutrino detection have been discussed in the literature [2–11].

In the present work we propose a new experimental method using excited atomic targets. The idea is based on the fact that radiative emission of neutrino pairs (RENP) [12,13] is affected by the Pauli blocking of ambient cosmic neutrinos [14]. We shall give an answer to the fundamental issue of how sensitive the Pauli blocking effect is to determination of cosmological parameters, the neutrino temperature, and the chemical potential which is related to the lepton asymmetry of our Universe.

The process we use is atomic deexcitation from a metastable state $|e\rangle$: $|e\rangle \to |g\rangle + \gamma + \nu_i\bar{\nu}_j$ (antineutrino $\bar{\nu}_j$ is identical to ν_j in the case of Majorana neutrino). The energy spectrum of the photon γ and parity violating quantities such as the asymmetry of rates under the magnetic field reversal [15] are measured in RENP. $\nu_i (i = 1, 2, 3)$ is a mass eigenstate of neutrinos and a mixture of neutrino species ν_e, ν_μ, ν_τ that appear in the weak decay of elementary particles. Neutrino oscillation experiments [16] have determined two mass squared differences, $(\sim 50\ \text{meV})^2$ and $(\sim 10\ \text{meV})^2$, and three mixing angles in a theoretical framework of an extended standard gauge theory where finite neutrino masses and 3×3 unitary mixing are introduced as an extra assumption—the crucial departure from the standard theory framework. The RENP process predicts a continuous photon energy spectrum at $\omega < \omega_{ij}$ (we use the natural unit of $\hbar = c = k_B = 1$ such that ω is the photon energy). Six thresholds are given by $\omega_{ij} = \epsilon_{eg}/2 - (m_i + m_j)^2/(2\epsilon_{eg})$ with ϵ_{eg} the level spacing of excitation. Since RENP occurs via stimulated photon emission by trigger lasers, decomposition into neutrino mass eigenstates is made possible by the excellent resolution of trigger laser frequencies.

The RENP experimental project [13] has been proposed for several objectives related to neutrino physics, in particular, to determine the smallest neutrino mass m_0, to distinguish the Majorana neutrino from the Dirac neutrino, and to determine the remaining elements of the mixing matrix, the CP violating (CPV) phases including the ones intrinsic to the Majorana neutrino. Since the weak process involves the Fermi constant G_F of inverse energy squared dimensions, the weak process rates are usually small for small available energies such as atomic deexcitation. The important concept of macrocoherence was introduced [13,17] to enhance otherwise small rates, extending the idea of Dicke's super-radiance [18]. This is a cooperative and coherent amplification extended over a macroscopic body. The macrocoherence concept [17] gives the dependence of rates $\propto n^3 V$, with n the target number density and V the target volume, as well as the phase matching condition or the momentum conservation among three light particles $\gamma, \nu_i, \bar{\nu}_j$ [19]. The macrocoherence works when more than two light particles are emitted in the final state, giving an important difference from the super-radiance of a single-photon emission that restricts

*yoshim@okayama-u.ac.jp
†sasao@okayama-u.ac.jp
‡tanaka@phys.sci.osaka-u.ac.jp

the coherent region to wavelength squared if all the laser irradiation is uniaxial [18].

Recently, our group succeeded in experimentally observing the macrocoherent two-photon emission of a weak QED process called paired super-radiance (PSR) [20]. This indicates the enhancement mechanism ($>10^{15}$ enhancement in rate) of macrocoherence. The degree of macrocoherence is determined to be large, of order ~6% averaged over a macroscopic target of 15 cm length, by comparison with detailed simulations [21]. A similar, but larger, macrocoherence should also work in RENP.

Under the ambient relic neutrino background RENP rates are reduced by the product of Pauli blocking factors $(1-f_i)(1-\bar{f}_j)$ where $f_i, \bar{f}_j$ are the momentum distribution functions for mass eigen-states $\nu_i, \bar{\nu}_j$. The Einstein relation in the expanding universe is $E = \sqrt{p^2 + m^2/(z+1)^2}$, $z+1 = a(t)/a(t_d)$ where $a(t), t_d, z$ are the cosmic scale factor at the present time, at the decoupling time, and the redshift factor since the neutrino decoupling. To a good approximation (ignoring the momentum region, $p < O(100\ \text{meV})/(z+1) \sim O(10^{-11})$ eV of extremely small phase space), the neutrino mass term can be neglected in the distribution functions even at the present epoch. Physically, this means that observable relic neutrinos at the present epoch were highly relativistic at decoupling. The distribution function after the neutrino decoupling changes under the gravity of the expanding universe and its present form are given by $f_i(p) = 1/(e^{p/T_\nu - \mu_d/T_d} + 1)$ where T_ν is the effective neutrino temperature at present given by $(4/11)^{1/3} T_\gamma \sim 1.9$ K. The quantity related to the chemical potential, μ_d/T_d, is the ratio of the chemical potential to the temperature at the epoch of neutrino decoupling [22]. For $\bar{\nu}_j$ the chemical potential is sign reversed: $\mu_d \to -\mu_d$. The upper bound allowed by nucleosynthesis is $\sim O(0.1)$ [23]. Some cosmological models predict a large μ_d/T_d [24].

The underlying assumption for description in terms of a single neutrino temperature T_ν is that no dramatic entropy generation occurs at the epoch between decoupling of ν_μ, ν_τ and the electron neutrino ν_e, since their decoupling temperatures are close: ~1.9 MeV for ν_e decoupling and ~3.1 MeV for ν_μ, ν_τ decoupling [25]. The measurement of 1.9 K neutrino temperature different from the microwave temperature 2.7 K is a clear indication of a physical process that occurred at earlier epochs of a few seconds after the big bang: electron-positron annihilation [1].

Weak interaction in the standard gauge theory has different strengths for different helicities or chiralities of neutrinos. This gives different decoupling epochs, hence, different temperatures, in principle, for neutrinos of different helicities. Despite this, in the present calculation we use helicity summed rates of neutrino pair production given in [7] and the same neutrino temperature for different helicity states. This is allowed if no significant entropy production occurs at the epoch between two different neutrino decoupling times. Results in this case agree with those of 1.9 K in the figures below. A more suitable analysis would be to assume two different neutrino temperatures and leave the temperature of the right-handed neutrino as a free parameter (the other fixed by 1.9 K) and use production rates for different helicity combinations employing different Pauli blocking factors. Indication of a neutrino temperature much below 1.9 K may be taken as an implication that the new physics scale is much above the Fermi scale of a fraction of 1 TeV.

The effect of the gravitational clustering is expected to be small in the neutrino mass range of $<O(100)$ meV considered below. The gravitational clustering of massive neutrinos enhances distortion of the spectrum further than the case without clustering, thus, giving a brighter prospect for relic neutrino detection. A simple rough estimate of the clustering effect is to multiply the ratio of the number density of relevant neutrinos in our galaxy to the cosmic density $3\zeta(3)T_\nu^3/(2\pi^2) \sim 110\ \text{cm}^{-3}$. This ratio may be calculated by solving the gravitational collapse of massive but noninteracting particles under the gravity of cold dark matter [26,27].

Spectrum shape functions previously derived without the Pauli blocking effect [28,29] are modified by $(1-f_i)(1-\bar{f}_j)$ for pair production of $\nu_i \bar{\nu}_j$ at $\omega < \omega_{ij}$. The spectral shape function F^A ($A = M$ for the nuclear monopole contribution of three thresholds ω_{ii} [28] and $A = S$ for the electron spin contribution of much smaller absolute rates [29], two cases being applicable to atoms of different quantum numbers) for the neutrino pair production of masses m_i, m_j is calculated as an integral over one of the neutrino energies,

$$F_{ij}^A(\omega; T_\nu) = \frac{1}{8\pi\omega} \int_{E_-}^{E_+} dE_1 g_{ij}^A(E_1) \cdot \left(1 - f(\sqrt{E_1^2 - m_i^2}))(1 - \bar{f}(\sqrt{(\epsilon_{eg} - \omega - E_1)^2 - m_j^2})\right), \tag{1}$$

$$g_{ii}^M(E) = -E^2 + (\epsilon_{eg} - \omega)E + \frac{1}{2}m_i^2 - \frac{1}{4}\epsilon_{eg}(\epsilon_{eg} - 2\omega) + \delta_M \frac{m_i^2}{2}, \tag{2}$$

$$g_{ij}^S(E) = -\frac{1}{3}E^2 + \frac{1}{3}(\epsilon_{eg} - \omega)E + \frac{1}{12}\epsilon_{eg}(\epsilon_{eg} - 2\omega) - \frac{1}{12}(m_i^2 + m_j^2) - \delta_M \frac{m_i m_j}{2}, \tag{3}$$

$$E_{\pm} = \frac{1}{2}\left((\epsilon_{eg} - \omega)\left(1 + \frac{m_i^2 - m_j^2}{\epsilon_{eg}(\epsilon_{eg} - 2\omega)}\right) \pm \omega\Delta_{ij}(\omega)\right), \qquad \Delta_{ij}(\omega) = \left\{\left(1 - \frac{(m_i + m_j)^2}{\epsilon_{eg}(\epsilon_{eg} - 2\omega)}\right)\left(1 - \frac{(m_i - m_j)^2}{\epsilon_{eg}(\epsilon_{eg} - 2\omega)}\right)\right\}^{1/2}, \tag{4}$$

times factors related to atomic matrix elements and energy denominators in perturbation theory [13]. These atomic factors cancel out in the ratio of rates, the rate with to the rate without the Pauli blocking. Equation (1) is a function of photon energy ω, depending on five parameters, two cosmological ones $T_\nu, \mu_d/T_d$, two neutrino masses, m_i, m_j, and the atomic level spacing ϵ_{eg}. $\delta_M = 1$ for Majorana neutrinos, arising from the interference term of identical fermions, and $\delta_M = 0$ in its absence for Dirac neutrinos. In the numerical calculations below, we present results for the Majorana case. One may define the total ratio adding all pair threshold contributions with weights determined by oscillation data [16]; $R_A(\omega) = F^A(\omega; T_\nu)/F^A(\omega; 0)$ ($F^A(\omega; 0)$ is the rate factor without the Pauli blocking). The theoretically calculated quantity $R_A(\omega)$ shown below is sensitive to ϵ_{eg} and to no other atomic parameters. Corresponding experimental values $R_A(\omega)$ need the input of the theoretical calculation of rates without Pauli blocking, which requires other atomic parameters than ϵ_{eg}.

Calculated theoretical values of the spectral distortion are shown in Fig. 1, Fig. 2, and Fig. 4 for the nuclear monopole contribution and in Fig. 3 for the spin current contribution. Effects of nonvanishing CPV phases that appear in the weight factor of pair emission are small; hence, for simplicity, we assume the vanishing CPV phase in the following analysis. Main results shown in Figs. 1 and 4, but not in Figs. 2 and 3, are insensitive to which of the neutrino mass hierarchical patterns—the normal (NH) or inverted hierarchy (IH) [16]—is adopted, and results for these two cases are identical.

The Pauli blocking effect becomes the largest in the threshold region of neutrino pair emission of smallest mass m_0. Since we explore the sensitivity to target properties, we study distortion effects by making the level spacing ϵ_{eg} as a free parameter. In Figs. 1–4, we take hypothetical atoms of excitation energy in the range 0.1–100 meV and show the Pauli blocking effect given by the rate ratio $R_A(\omega)$. The difference between distortions of 1.9 and 2.7 K, the important issue in cosmology, may reach the 10% level for an appropriate combination of m_0 and ϵ_{eg}, as in Fig. 1.

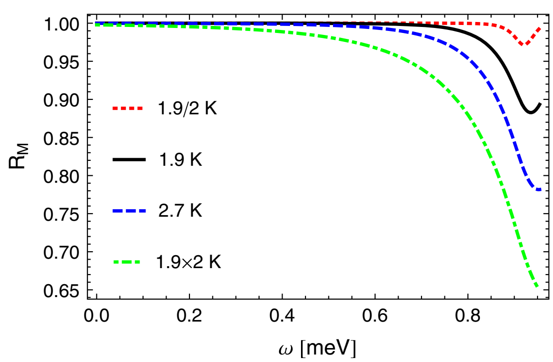

FIG. 1 (color online). Spectral distortion $R_M(\omega)$ caused by the Pauli blocking of relic neutrinos, $T_\nu = 1.9/2$ K in dotted red, 1.9 K in solid black, 2.7 K in dashed blue, and 1.9×2 K in dash-dotted green, all assuming $m_0 = 5$ meV, $\epsilon_{eg} = 11$ meV, and the zero chemical potential. Distortions are identical for the two cases of NH and IH.

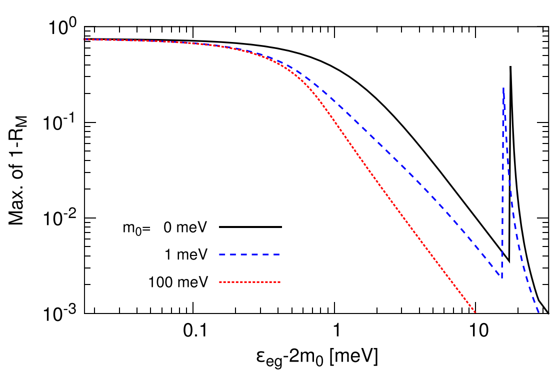

FIG. 2 (color online). Maxima of the spectral deviation $1 - R_M(\omega)$ caused by the Pauli blocking plotted against the difference between level splitting and twice of the lightest neutrino mass, $\epsilon_{eg} - 2m_0$. We show the cases of NH $m_0 = 0$ meV (solid black), NH 1 meV (dashed blue) and NH 100 meV (dotted red), assuming the zero chemical potential.

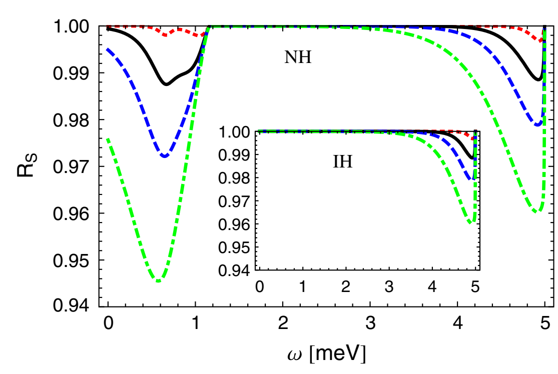

FIG. 3 (color online). Spectral distortion $R_S(\omega)$ caused by the Pauli blocking. $T_\nu = 1.9/2$ K in dotted red, 1.9 K in solid black, 2.7 K in dashed blue, and 1.9×2 K in dash-dotted green, all assuming $m_0 = 0.1$ meV, $\epsilon_{eg} = 10$ meV, and the zero chemical potential. IH case is shown in the inset for comparison with NH case.

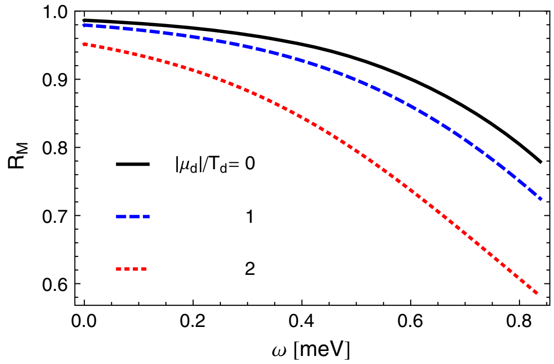

FIG. 4 (color online). Spectrum distortion $R_M(\omega)$ for magnitudes of neutrino degeneracy $|\mu_d|/T_\nu = 0$ in solid black, 1 in dashed blue, and 2 in dotted red. The lightest neutrino mass $m_0 = 0$ meV is taken. $\epsilon_{eg} = 10T_\nu \sim 1.7$ meV chosen.

Study of relic neutrino detection becomes more practical after the RENP process is discovered for a definite target atom and a range of smallest neutrino mass is identified. Anticipating an approximate m_0 determination already achieved, we present in Fig. 2 the maximal spectral distortion assuming a special relation between m_0 and the atomic level spacing. The peak structure for m_0 values of 0, 1 meV observed in Fig. 2, which shows a large distortion, is due to the second threshold ω_{22} of the next-lightest neutrino pair of mass $\sim$10 meV.

At the zero momentum limit of $p = 0$, $1 - f_i \sim 1/2$ with the vanishing chemical potential, and the effect of Pauli blocking becomes the largest [7]. The reason the largest distortion of 3/4 is not realized in RENP is that at thresholds ω_{ij}, neutrinos cannot carry the zero momentum and only a partial blocking occurs, since the half energy $\sim\epsilon_{eg}/2$ is shared by two neutrinos.

The absolute value of RENP spectral rates depends linearly on a time-varying dynamical factor $\eta_\omega(t)$, which is the product of medium polarization and the stored field energy in dimensionless units and may be calculated by solving the master equation of coherence evolution [13]. $\eta_\omega(t)$ values can be as large as 10^{-3} (see below). The nuclear monopole contribution [28] is a nuclear coherent effect caused by the Z boson exchange between quarks in nuclei and neutrinos, which is dominantly given by the electroweak charge $Q_w = N - (1 - 4\sin^2\theta_w)Z$, with N, Z the neutron number and the proton number of the nucleus of the four-vector part of the currents for heavy nuclei. The rate is further enhanced by a large Coulomb interaction, giving the dependence $Q_w^2 Z^{8/3}$ for rates. A similar coherent effect works for the enhanced amplitudes of atomic parity violation experiments [30]. The nuclear monopole contribution gives the largest rate of order 50 events/second $\times\, \eta_\omega(t)$ at its maximum for Xe atomic deexcitation of $^3P_1(\sim 8.4$ eV) for a gas target number density $7\times 10^{19}\,\mathrm{cm}^{-3}$ and a target volume 10^2 cm^3. Dependence on atomic parameters is more complicated, but very roughly the rate scales as $\propto$ the level spacing $\epsilon_{eg} \times$ relevant E1 dipole strength squared. Although the rate near the threshold is suppressed, it rapidly increases towards a maximum value at higher photon energies, much like in the muon decay into three light leptons.

Distortions of 10% or more seen in Fig. 1 and Fig. 2 for the nuclear monopole contribution are experimentally encouraging. The distortion of the photon spectrum in the spin current contribution has an interesting second structure as shown in Fig. 3 due to the second threshold of the neutrino pair of smallest and next-smallest masses. This second structure is present only in the NH case. Rates are, however, much smaller than in the monopole case [28].

The distorted spectrum for a finite value of the chemical potential has been calculated as illustrated in Fig. 4. For a choice of small m_0, effects of the finite chemical potential may be non-negligible.

Finally, we mention the directional variation of the distorted spectrum. This is caused by the earth motion relative to the 2.7 K microwave isotropic distribution, giving an effective momentum change of a dipole form in the neutrino distribution function of order given by its velocity $v/c = O(10^{-3})$. This effect should help identify relic RENP events near the thresholds.

The prospect of relic neutrino detection is closely tied to the success of neutrino mass spectroscopy using RENP. The first important experimental step is to prove the new concept of macrocoherence. As mentioned above, we recently achieved the macrocoherence amplification in a weak QED process of PSR [20]. Moreover, the macrocoherent PSR may be used for development of the macrocoherence of RENP, which ultimately leads to formation of a static object called a soliton condensate [31], a two-photon analogue of stopped light to the familiar electric dipole transition [32]. This is the remnant state of a large stored light field coupled to a macroscopic medium polarization after the termination of PSR-related activity, giving a stationary value for the dynamical factor η_ω (that remains after extraction of $\propto n^3V$ dependence) as large as 10^{-3} or even greater [13]. In the target state of soliton condensates, two-photon QED backgrounds are exponentially suppressed, thus enhancing the signal-to-background ratio [31]. It is, thus, crucial to control PSR and promote the soliton formation process by experimental means. Since initial states for PSR and RENP processes have different parities, one needs a switching mechanism between two different parities. One of the ideas for this is the use of the external electric field to mix different parity states. The experimental study of targets in solid environments is important to further define a practical way to conduct the RENP experiment.

The important idea of the soliton condensate has been studied extensively in the usual electric dipole transition under the name "polariton" [33]. This is a coherent state of target in which the light electric field is strongly coupled with atomic macroscopic polarization and forms a joint eigenstate. The light field can be stored within a target by a large amount and, in special cases, the light field apparently does not move at all: stopped light. Needless to say, this is achieved by the supporting system of atomic polarization, and one may regard the event as a continuous process of emission and absorption occurring always within a target. Our soliton condensate is two-photon analogue of the stopped light and is yet to be discovered experimentally, although its existence has been shown even in the presence of relaxation [31]. An important outcome of the stopped light in the two-photon case is that light can escape the target only from its ends, with an exponentially suppressed rate. This feature of suppressed photon emission is very useful to reduce QED backgrounds against RENP since the RENP process can occur perturbatively from the bulk of the target with no suppression at all.

We have a comment on the background against RENP. Stimulated QED backgrounds could seriously impact RENP. We have a workable idea, which will be discussed in a separate publication, to reject this background altogether by putting the target inside a wave guide. A practical experimental proposal of relic neutrino detection should be prepared only after one knows the smallest neutrino mass with some precision. How much and what kind of lasers should be used for excitation and triggering can be determined only after we decide a target atom for RENP.

In summary, neutrino mass spectroscopy using RENP may become a sensitive tool to explore the early cosmic epoch at the decoupling of the electron neutrino. We proposed to use distortion of the photon energy spectrum caused by the Pauli blocking of ambient relic neutrinos. The sensitivity to the background temperature measurement depends on the unknown mass value of the lightest neutrino, in relation to the level spacing of excitation. The spectrum distortion may become large, significantly more than the 10% level along with this order of temperature distinction of 1.9 and 2.7 K. A small level spacing, thus favored, may be provided by fine structure splitting of atoms or in molecular rotational transitions.

We would like to thank K. Inoue and M. Yamaguchi at Tohoku University for valuable discussions. This research was partially supported by a Grant-in-Aid for Scientific Research on Innovative Areas," Extreme quantum world opened up by atoms," (No. 21104002) from the Ministry of Education, Culture, Sports, Science, and Technology, and JSPS KAKENHI Grant No. 25400257.

Note added in proof.—We worked out in [34] how stimulated QED backgrounds are eliminated in RENP, when targets are put in wave guide or photonic crystal type fibers, as mentioned in the present work.

[1] For a comprehensive overview of big bang cosmology and nucleosynthesis, see the textbook, S. Weinberg, *Gravitation and Cosmology* (John Wiley and Sons, New York, 1972).

[2] S. Weinberg, Phys. Rev. **128**, 1457 (1962).

[3] P. Langacker, J. P. Leveille, and J. Sheiman, Phys. Rev. D **27**, 1228 (1983), and references therein; N. Cabbibo and L. Maiani, Phys. Lett. **114B**, 115 (1982).

[4] L. Stodolsky, Phys. Rev. Lett. **34**, 110 (1975).

[5] T. J. Weiler, Phys. Rev. Lett. **49**, 234 (1982).

[6] J. M. Irvine and R. Humphreys, J. Phys. G **9**, 847 (1983).

[7] T. Takahashi and M. Yoshimura, Effect of Relic Neutrino on Neutrino Pair Emission from Metasable Atoms, arXiv: hep-ph/0703019v1.

[8] R. S. Raghavan, arXiv:hep-ph/0703028.

[9] A. G. Cocco, G. Mangano, and M. Messina, J. Cosmol. Astropart. Phys. 06 (2007) 015; arXiv:hep-ph/0703075v1.

[10] For earlier reviews of relic neutrino detection, see G. Gelmini, Phys. Scr. **T121**, 131 (2005); A. Ringwald, Nucl. Phys. **A827**, 501c (2009).

[11] On the PTOLEMY project, see S. Betts *et al.*, arXiv: 1307.4738v2.

[12] M. Yoshimura, Phys. Rev. D **75**, 113007 (2007).

[13] A. Fukumi *et al.*, Prog. Theor. Exp. Phys. (**2012**) 04D002, and earlier references cited therein.

[14] In [7] the inverse process of $\gamma + |g\rangle \to \nu_i\bar{\nu}_j + |e\rangle$ to RENP was considered, taking into account the Pauli blocking effect. The process is more difficult to experimentally detect than RENP, even if it can be macro-coherently amplified. But the Pauli blocking effect is larger and reaches the largest reduction factor $3/4$ in the range $m_0 \leq 1$ meV even for larger level spacing ϵ_{eg}.

[15] M Yoshimura, N. Sasao, and S. Uetake, Phys. Rev. D **90**, 013022 (2014).

[16] G. L. Fogli, E. Lisi, A. Marrone, D. Montanino, A. Palazzo, and A. M. Rotunno, Phys. Rev. D **86**, 013012 (2012); M. C. Gonzalez-Garcia, M. Maltoni, J. Salvado, and T. Schwetz, J. High Energy Phys. 12 (2012) 123; D. V. Forero, M. Toacutertola, and J. W. F. Valle, Phys. Rev. D **86**, 073012 (2012).

[17] M. Yoshimura, N. Sasao, and M. Tanaka, Phys. Rev. A **86**, 013812 (2012).

[18] R. H. Dicke, Phys. Rev. **93**, 99 (1954).

[19] An intuitive way of understanding the macrocoherence is as follows. Suppose that we calculate a total rate of the collective body of excited atoms given by a formula, $|\sum_a e^{i(\vec{k}+\vec{p}_1+\vec{p}_2)\cdot\vec{r}_a}\mathcal{M}_a|^2$, where emitted plane waves at the atomic site $\vec{r}_a$ are explicitly written. If the atomic phase relaxation at different atomic sites is slow in time and atomic matrix elements $\mathcal{M}_a$ are spatially slowly varying, then one may factor out this part of the matrix elements, to obtain the above formula $= (2\pi)^3\delta(\vec{k} + \vec{p}_1 + \vec{p}_2)n^2V|\mathcal{M}|^2$, where n is

the number density of excited atoms in the coherent volume V. An extra n factor of $\propto n^3 V$ dependence arises from the stored field, since the process is stimulated by the stored field.
[20] Y. Miyamoto *et al.*, Prog. Theor. Exp. Phys. (**2014**) 113C01.
[21] We use in our numerical simulations the Maxwell-Bloch equation (equivalent to the Maxwell-Schrodinger equation) in one space and one time dimension relevant to the laser irradiation, including a general form of relaxation constant appropriate to a reduced two-level system. If the phase relaxation time is large enough (as in our experimental system), an initial coherence between two levels imprinted by a high-quality laser excitation (as in our experiment) develops to a macrocoherence necessary for a large enhancement of the effective rate. Once the macrocoherence works, the rate becomes $\propto n^3 V$ according to the arguments of [19].
[22] One might consider that the chemical potential is defined only in the case of the Dirac neutrino in which the particle number is well defined. But weak interaction of the Majorana neutrino prior to decoupling distinguishes two different helicity states, which may effectively be regarded as particle and antiparticle as in the Dirac case. Only the gravitational clustering that occurs much later mixes two helicity states, thereby making the chemical potential vanishing. Since we do not need to consider the effect of gravitational clustering, even the Majorana case may be endowed with the chemical potential.
[23] R. V. Wagoner, W. A. Fowler, and F. Hoyle, Astrophys. J. **148**, 3 (1967); Y. David and H. Reeves, Phil. Trans. R. Soc. A **296**, 415 (1980); N. C. Rana, Phys. Rev. Lett. **48**, 209 (1982); H. Kang and G. Steigman, Nucl. Phys. **B372**, 494 (1992); D. J. Schwarz and M. Stuke, New J. Phys. **15**, 033021(2013).
[24] Examples giving a large lepton asymmetry are A. Casas, W. Y. Cheng, and G. Gelmini, Nucl. Phys. **B538**, 297 (1999); J. McDonald, Phys. Rev. Lett. **84**, 4798 (2000).
[25] A. D. Dolgov, Phys. Rep. **370**, 333 (2002).
[26] S. Singh and C. P. Ma, Phys. Rev. D **67**, 023506 (2003).
[27] A. Ringwald and Y. Wong, J. Cosmol. Astropart. Phys. 12 (2004) 005.
[28] M. Yoshimura and N. Sasao, Phys. Rev. D **89**, 053013 (2014).
[29] D. N. Dinh, S. Petcov, N. Sasao, M. Tanaka, and M. Yoshimura, Phys. Lett. B **719**, 154 (2013).
[30] M. A. Bouchiat *et al.*, Phys. Lett. **134B**, 463 (1984), and references therein; P. S. Drell and E. D. Commins, Phys. Rev. A **32**, 2196 (1985), and references therein; M. C. Noecker, B. P. Materson, and C. E. Wieman, Phys. Rev. Lett. **61**, 310 (1988), and references therein.
[31] M. Yoshimura and N. Sasao, Prog. Theor. Exp. Phys. (**2014**) 73B02.
[32] G. Heinze, C. Hubrich, and T. Halfmann, Phys. Rev. Lett. **111**, 033601 (2013), and references therein.
[33] J. Kasprzak *et al.*, Nature (London) **443**, 409 (2006); R. Balili, V. Hartwell, D. Snoke, L. Pfeiffer, and K. West, Science **316**, 1007 (2007); For introduction of cavity polaritons, see for example, A. Kavokin and G. Malpuech, *Thin Films and Nanostructures: Cavity Polaritons* (Elsevier, New York, 2003).
[34] M. Yoshimura, N. Sasao, and M. Tanaka, arXiv:1501.05713